SCIENTIFIC REPORTS
nature research

Check for updates

OPEN

Crystal and Magnetic Structures of Double Hexagonal Close-Packed Iron Deuteride

Hiroyuki Saitoh[1]✉, Akihiko Machida[1], Riko Iizuka-Oku[2], Takanori Hattori[3], Asami Sano-Furukawa[3], Ken-ichi Funakoshi[4], Toyoto Sato[5], Shin-ichi Orimo[5,6] & Katsutoshi Aoki[2]✉

Neutron powder diffraction profiles were collected for iron deuteride (FeD_x) while the temperature decreased from 1023 to 300 K for a pressure range of 4–6 gigapascal (GPa). The ε′ deuteride with a double hexagonal close-packed (dhcp) structure, which coexisted with other stable or metastable deutrides at each temperature and pressure condition, formed solid solutions with a composition of $FeD_{0.68(1)}$ at 673 K and 6.1 GPa and $FeD_{0.74(1)}$ at 603 K and 4.8 GPa. Upon stepwise cooling to 300 K, the D-content *x* increased to a stoichiometric value of 1.0 to form monodeuteride $FeD_{1.0}$. In the dhcp $FeD_{1.0}$ at 300 K and 4.2 GPa, dissolved D atoms fully occupied the octahedral interstitial sites, slightly displaced from the octahedral centers in the dhcp metal lattice, and the dhcp sequence of close-packed Fe planes contained hcp-stacking faults at 12%. Magnetic moments with 2.11 ± 0.06 μ_B/Fe-atom aligned ferromagnetically in parallel on the Fe planes.

Iron (Fe) reacts with hydrogen (H) to form solid solution FeH_x or stoichiometric monohydride $FeH_{1.0}$ at hydrogen pressures (hereafter referred to simply as *pressure*) in a gigapascal (GPa) range. Because of a prototypical transition-metal hydride, structural and physical properties have been intensively investigated for the Fe–H system over the past 50 years[1–20]. In temperature–pressure (*T*–*P*) ranges of 0–2000 K and 0–10 GPa, three solid phases (α, ε′, and γ phases) are present: the α phase with a body-centered cubic (bcc) structure, the ε′ phase with a double hexagonal close-packed (dhcp) structure, and the γ phase with a face-centered cubic (fcc) structure[2,8,10]. These phases join at a triple point at ~570 K and ~5.0 GPa[7,10]. In each hydride, dissolved H atoms, partially or fully occupying the interstitial sites of a host metal lattice, cause the metal lattice to expand and provide a certain amount of electrons to the metal lattice[1,6,14,18]. Thus, hydrogenation is an effective means for creating or modifying the physical properties while maintaining the structure of the metal lattice.

The ε′ phase exhibits unique structural and physical properties, e.g., extensive stability, stoichiometric composition, and ferromagnetism. The phase diagram of the Fe–H system extending to 3000 K and 120 GPa indicates the ε′ phase as the only stable phase at pressures greater than 20 GPa, presumably maintaining the stoichiometric composition of $FeH_{1.0}$[12]. Such unique phase stability allows for the investigation of the structural and magnetic properties over a wide *T*–*P* range. Ferromagnetic–paramagnetic transition has been experimentally investigated at ambient temperature and pressure up to 80 GPa by Mössbauer (MB) and X-ray magnetic circular dichroism (XMCD) spectroscopies[21–23]. These results showed that the magnetic moment of dhcp $FeH_{1.0}$ continuously deceased with pressure and eventually disappeared at roughly 30 GPa at 300 K. The magnitude and alignment of the magnetic moments have been theoretically predicted at 0 K and ambient pressure using density-functional theory (DFT) calculations of the electronic band structure[24–28].

Two essential subjects regarding the ε′ phase remain uninvestigated. First, the magnetic structure should be determined experimentally although the ferromagnetism has been confirmed by MB, XMCD, and magnetization measurements[21–23,29–34]. Neutron powder diffraction (NPD) measurements were carried out for quenched

[1]Quantum Beam Science Research Directorate, National Institutes for Quantum and Radiological Science and Technology, 1-1-1, Kouto, Sayo-cho, Sayo-gun, Hyogo, 679-5148, Japan. [2]Geochemical Research Center, Graduate School of Science, The University of Tokyo, 7-3-1 Hongo, Bunkyo-ku, Tokyo, 113-0033, Japan. [3]J-PARC Center, Japan Atomic Energy Agency, Tokai, Naka, Ibaraki, 319-1195, Japan. [4]Neutron Science and Technology Center, Comprehensive Research Organization for Science and Society, Shirakata, 162-1, Shirakata, Tokai, Naka, Ibaraki, 319-1106, Japan. [5]Institute for Materials Research, Tohoku University, 2-1-1 Katahira, Aoba-ku, Sendai, 980-8577, Japan. [6]WPI-Advanced Institute for Materials Research (AIMR), Tohoku University, 2-1-1, Katahira, Aoba-ku, Sendai, 980-8577, Japan. ✉e-mail: saito.hiroyuki@qst.go.jp; k-aoki@eqchem.s.utokyo.ac.jp

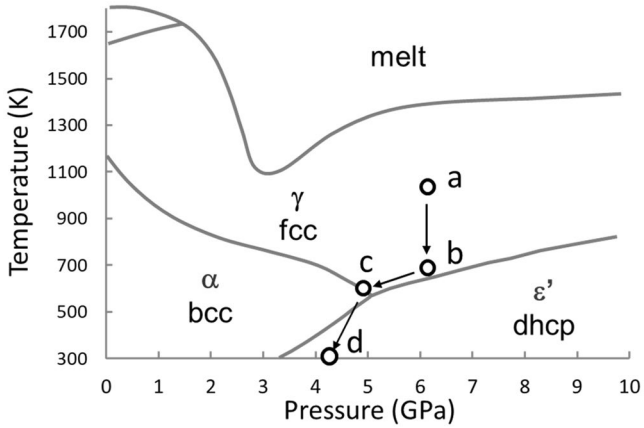

Figure 1. Phase diagram of the Fe–H system redrawn from[10]. A triple point is located at ~570 K and ~5.0 GPa. Open circles denote the *T*–*P* points of NPD measurements: (**a**) 1023 K and 6.1 GPa, (**b**) 673 K and 6.1 GPa, (**c**) 603 K and 4.8 GPa, and (**d**) 300 K and 4.2 GPa.

deuterides/hydrides containing the ε′ phase as a major component[6]. The crystal structure, including the H/D atomic positions, was precisely determined, but the magnetic structure was not determined because of the weak magnetic scattering intensities. Second, the H content x is unknown for the high-temperature solid solution. The dhcp hydride has been considered to maintain $x = 1.0$ across almost the entire stable *T*–*P* range[1]. The most recent X-ray diffraction measurements revealed a substantial reduction in volume at high temperatures near the dhcp–fcc phase boundary, and the partial release of dissolved H atoms or the formation of the solid solution was suggested in this regard[16].

We carried out *in situ* NPD measurements on FeD_x in the *T*–*P* ranges of 300–1023 K and 4.2–6.1 GPa. The crystal and magnetic structures were refined for the dhcp deuteride using the model structures proposed in the early NPD study[6] and predicted in the electronic band structure calculation[26]. The structure of dhcp $FeD_{1.0}$ contained the off-central displacement of D atoms on octahedral interstitial sites and stacking faults in the dhcp sequence of Fe planes, consistent with the early results[6]. The atomic displacement and the stacking faults were partially or fully removed in the solid-solution states at high temperatures. The magnitude and alignment of the magnetic moments were in agreement with those theoretically calculated for ferromagnetic dhcp $FeH_{1.0}$[26].

Results

NPD profiles were collected for the Fe deuteride at four *T*–*P* points (Fig. 1). The fcc solid solution was first prepared by deuterization of fcc Fe at 1023 K and 6.1 GPa and then cooled to 673 K, where the fcc deuteride partially transformed to the dhcp deuteride along with the formation of a small amount of a metastable hcp modification. The measured *T*–*P* point was located immediately above the γ–ε′phase boundary and was considered to be still within the stable range of the γ phase. The latest NPD study of Fe hydride revealed that the γ–ε′phase boundary was located at temperatures 100–200 K higher than those shown in Fig. 1[19], and the appearance of the dhcp deuteride at 673 K and 6.1 GPa was consistent with the latest result. The formation of the metastable hcp phase was sensitive to the cooling rate; a larger amount of the hcp deuteride formed at a faster cooling rate[18]. The cooling rate was gradually decreased from 10 K/min to 1 K/min. The hcp formation, however, was not completely prevented. The coexisting state of the dhcp, fcc, and hcp deuterides was retained at 603 K and 4.8 GPa. When the temperature was decreased to 300 K, the hcp deuteride decomposed to dhcp monodeuteride and bcc Fe, whereas the dhcp and fcc deuteride remained almost unchanged.

The observed diffraction profiles were simulated using model structures proposed for dhcp[6], fcc[14], and hcp hydrides/deuterides[18] in early NPD studies. Dissolved D atoms were located on the centers of the octahedral and tetrahedral interstitial sites (hereafter, referred to as the O site and T site, respectively) of the fcc and hcp metal lattices, whereas they were located on the off-centered positions of the octahedra in the dhcp lattice. The crystal structure of dhcp $FeD_{1.0}$ used as the model structure is schematically shown in Fig. 2[6]. This structure belongs to the $P6_3/mmc$ space group and has the stacking sequence of the Fe planes, ABACA⋯, which comprises "hexagonal" stacking of ABA or ACA and "cubic" stacking of BAC. Figure 2b shows the spatial configuration of the Fe octahedra available for accommodating D atoms, and the octahedra are connected in a face-shared configuration in the hexagonal stacking sequence and an edge-shared configuration in the cubic stacking sequence. Two structural irregularities were considered in the refinement of the dhcp structure according to[6], i.e., the displacement of D atoms along the *c*-axis (δz) and the stacking fault of the Fe planes, which was described using f_{reg} and f_{def}, denoting occupancies on the regular sites equivalent to the (1/3, 2/3, 7/8) position and defect sites equivalent to the (1/3, 2/3, 1/8) position, respectively.

For ferromagnetic dhcp $FeD_{1.0}$, two possible structures, *in-plane* and *out-of-plane* models, were examined when refining the magnetic structure[6,26]. The magnetic moments on the Fe atoms lay parallel within the metal planes in the in-plane model, whereas they stand vertically on the metal planes in the out-of-plane model. The calculations of neutron scattering intensities for the two model structures showed that their contributions to peak intensities were limited approximately to the 100, 101, 004, and 102 peaks, and relative intensities were

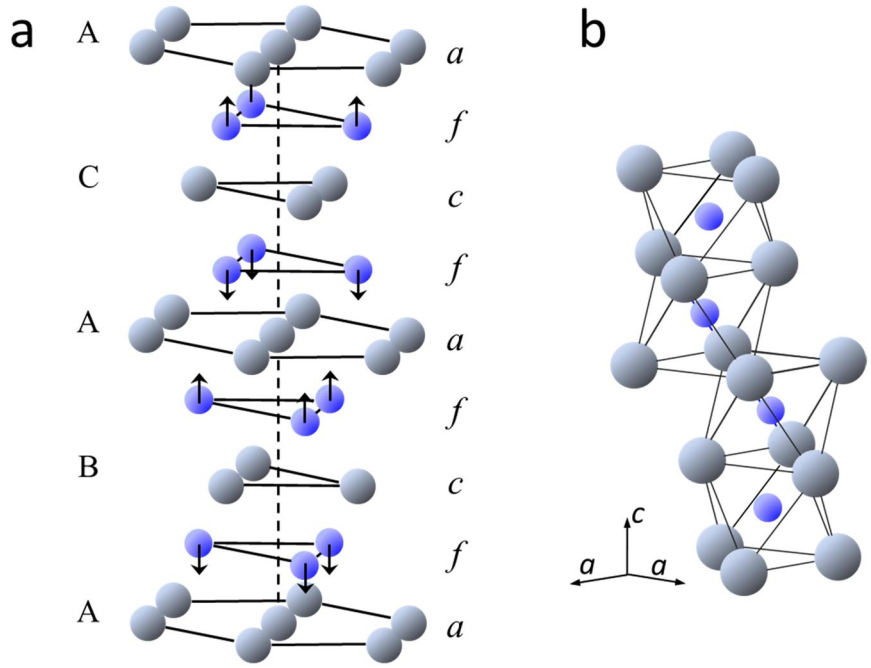

Figure 2. (**a**) Crystal structure of dhcp $FeD_{1.0}$ redrawn from[6]. Here, *a*, *c*, and *f* denote the planes of equivalent positions in the $P6_3/mmc$ space group that originated, respectively, from the positions 2*a*, 2*c*, and 4*f* with $z \approx 7/8$ (see Table 1). Gray and blue spheres indicate the regular positions of Fe and D atoms, respectively. Arrows indicate the directions of displacement of D atoms from the centers of octahedral interstices. Here, A, B, and C represent the standard notation for close-packed planes. (**b**) Face-shared octahedra accommodating D atoms.

substantially different between the two models[6]. These calculated peak intensities served as a guideline for the refinement of the magnetic structure in this study.

Figure 3 shows the observed diffraction profiles and their simulated profiles fitted by Rietveld refinement using a Z-Rietveld software (Version 1.1.2)[35]. As shown in Fig. 3a, the single-phase profile at 1023 K and 6.1 GPa was fitted with the fcc structure with a composition of $FeD_{0.62(3)}$ (hereafter, the numbers in parentheses denote experimental error). The profile at 673 K and 6.1 GPa had good a fit with the mixture of dhcp $FeD_{0.68(1)}$, hcp $FeD_{0.56(2)}$, and fcc $FeD_{0.59(1)}$, with mass ratios of $x_{mass} = 0.667(3)$, 0.171(2), and 0.162(2), respectively (Fig. 3b). The mass ratios slightly changed upon cooling to 603 K: $x_{mass} = 0.564(4)$ (dhcp), 0.277(4) (hcp), and 0.16 (fcc) (Fig. 3c). The diffraction profile at 300 K and 4.2 GPa was fitted with the mixture of dhcp $FeD_{1.0}$, fcc $FeD_{1.0}$, and bcc Fe at mass ratios of $x_{mass} = 0.708(4)$, 0.014(1), and 0.278(3), respectively (Fig. 3d).

Several fitting parameters were properly constrained to avoid convergence of the parameters into unphysical values. The atomic displacement parameters or temperature factors of D and Fe atoms were assumed equal among the coexisting deuterides. The occupancy ratio of f_{def}/f_{reg} was constrained to be equal between the Fe and D atoms in the refinement for the dhcp structure. The D composition was fixed at $x = 1.0$ for the dhcp and fcc deuterides in the refinement of the 300 K–4.2 GPa profile according to the early studies[6,16,18]. In addition, the magnetic moment of bcc Fe was fixed to an ambient pressure value of the 2.1 μ_B/Fe-atom (μ_B denotes the Bohr magneton). H atoms, which were included as an impurity by 4 atom% in the D source of AlD_3, were assumed to randomly occupy the D-atom sites. For the sake of simplicity, the site occupancies of H atoms and the H composition are included in the notations g_D and *x*, respectively.

For the dhcp $FeD_{1.0}$ at 300 K and 4.2 GPa, crystal structure including magnetic ordering was refined using the out-of-plane and in-plane models. In both models, one equivalent magnitude of magnetic moment was assumed. Figure 4 shows the fitting results obtained with (a) the nonmagnetic, (b) out-of-plane, and (c) in-plane models. The simulated profile of the nonmagnetic model showed substantial deficits in the intensities of the 100, 101, 004, and 102 peaks. A simulated profile for the out-of-plane model reproduced, with a reliability value of $\chi^2 = 11.3$, the observed intensities of the 101 and 102 peaks but failed to reproduce that of the 004 peak. The in-plane model yielded a slightly less value of $\chi^2 = 10.3$ and satisfactorily reproduced the intensities of all peaks with an optimized magnetic moment of 2.11(6) μ_B/Fe-atom. The rather high value of χ^2 arose from misfits in peak shape likely attributed to enhanced distortion of the dhcp Fe lattice by interstitial D atoms fully occupying the O sites.

The structure refinements included preferred-orientation correction for the *c* axis of the dchp lattice. *Pref. orient*. [001] is a parameter of the March-Dollase function implemented in the z-Rietveld program[35], and is optimized to reproduce peak intensities modified by the preferred orientation of the *c* axis. The structure refinement of dhcp FeD at 300 K and 4.2 GPa yielded *pref. orient*. [001] = 1.01. Calculations of peak intensities using a value of 1.01 and the March-Dollase function showed that the 100, 101, 004, and 102 peak intensities were modified by factors of 1.015 (+1.5%), 1.012 (+1.2%), 0.971(−2.9%), and 1.005 (+0.5%), respectively. These modification values are substantially less than the magnetic scattering components of the peak intensities as shown in Table 2

T, *P*, Reliable factors	Phase	Atom	Site	*x*	*y*	*z*	*B*(Å^2)	Occupancy
1023 K, 6.1 GPa R_{wp} = 10.2%, χ^2 = 1.12	fcc-$FeD_{0.62(3)}$, X_{mass} = 1.00 a = 3.70694(8)Å	Fe D D	4*a* 4*b* 8*c*	0 1/2 1/4	0 1/2 1/4	0 1/2 1/4	1.13(5) 3.3(1)	1.0 0.50(1) 0.06(1)
673 K, 6.1 GPa R_{wp} = 6.29%, χ2 = 4.42	dhcp-$FeD_{0.68(1)}$, X_{mass} = 0.667(3) a = 2.63677(8)Å, c = 8.6103(5)Å pref. orient. [001] = 1.11	Fe Fe D Fe D	2*a* 2c 4*f* 2*d* 4*f*	0 1/3 1/3 1/3 1/3	0 2/3 2/3 2/3 2/3	0 1/4 0.8767(4) 3/4 0.1233(4)	0.74(2) 2.15(7)	1.0 0.982(3) 0.670(6) 0.018(3) 0.012(1)
	hcp-$FeD_{0.56(2)}$, X_{mass} = 0.171(2) a = 2.6251(3)Å, c = 4.2478(11)Å pref. orient. [001] = 1.36	Fe D	2 *c* 2 *a*	1/3 0	2/3 0	1/4 0	0.74(2) 2.15(7)	1.0 0.56(2)
	fcc-$FeD_{0.59(1)}$, X_{mass} = 0.162(2) 3.72274(11)Å	Fe D D	4*a* 4*b* 8*c*	0 1/2 1/4	0 1/2 1/4	0 1/2 1/4	0.74(2) 2.15(7)	1.0 0.59(1) 0.0
603 K, 4.8 GPa R_{wp} = 7.16%, χ^2 = 3.38	dhcp-$FeD_{0.74(1)}$, X_{mass} = 0.564(4) a = 2.63759(8)Å, c = 8.6231(7) Å pref. orient. [001] = 1.22	Fe Fe D Fe D	2*a* 2c 4*f* 2*d* 4*f*	0 1/3 1/3 1/3 1/3	0 2/3 2/3 2/3 2/3	0 1/4 0.8818(5) 3/40.1182(5)	0.66(3) 1.93(7)	1.0 0.957(3) 0.716(6) 0.043(3) 0.028(1)
	hcp-$FeD_{0.44(1)}$, X_{mass} = 0.277(4) a = 2.61400(16)Å, c = 4.2464(6) Å pref. orient. [001] = 1.22	Fe D	2*c* 2*a*	1/3 0	2/3 0	1/4 0	0.66(3) 1.93(7)	1.0 0.44(1)
	fcc-$FeD_{0.46(1)}$, X_{mass} = 0.159(2) a = 3.7227(2)Å	Fe D D	4*a* 4*b* 8*c*	0 1/2 1/4	0 1/2 1/4	0 1/2 1/4	0.66(3) 1.93(7)	1.0 0.46(1) 0.0
300 K, 4.2 GPa R_{wp} = 10.6%, χ^2 = 10.3	dhcp-$FeD_{1.0}$, X_{mass} = 0.708(4) a = 2.66727(3)Å, c = 8.7277(3) Å pref. orient. [001] =1.01 μ_{mag} = 2.11(6) μ_B	Fe Fe D Fe D	2*a* 2c 4*f* 2*d* 4*f*	0 1/3 1/3 1/3 1/3	0 2/3 2/3 2/3 2/3	0 1/4 0.8803(2) 3/4 0.1197(2)	0.33(5) 0.96(2)	1.0 0.877(1) 0.877(1) 0.123(1) 0.123(1)
	fcc-$FeD_{1.0}$, X_{mass} = 0.014(1) a = 3.7800(7)Å	Fe D D	4*a* 4*b* 8*c*	0 1/2 1/4	0 1/2 1/4	0 1/2 1/4	0.33(5) 0.96(2)	1.0 1.0 0.0
	bcc-Fe, X_{mass} = 0.278(3) a = 2.84992(4)Å μ_{mag} = 2.1μ_B	Fe	2*a*	0	0	0	0.096(6)	1.0

Table 1. Structural parameters for dhcp, hcp, and fcc Fe deuterides, and bcc Fe optimized by Rietveld refinements. Here, *B* denotes isotropic atomic displacements in the unit of Å^2. The occupancy of Fe atoms at the 2*d* positions, which is denoted by f_{def} in the text, indicates the degree of stacking fault in the sequence of metal planes. The deviation of the *z*-position of D-atoms from 1/7 or 7/8 indicates off-centred displacement from the O-site centers, while μ_{mag} denotes magnetic moment for dhcp $FeD_{1.0}$ and bcc Fe. Reliability values of R_{wp} and χ^2 are also given. *Pref. orient.* [001] is a fitting parameter for reproducing peak intensities modified by the preferred orientation of the *c* axis.

in the following paragraph: for example, the 004 peak, with a maximum modification value of −2.9%, has a magnetic scattering component 57.1%. The parameter for preferred-orientation correction dose not significantly correlate with the Bragg intensities and hence its bias to the assignment of magnetic structure can be ruled out.

The fitting parameters optimized for the dhcp deuteride and the coexisting fcc and hcp deuterides, and bcc Fe are listed in Table 1. The contributions of nuclear scattering (I_{nuc}) and magnetic scattering (I_{mag}) to the intensities of the 100, 101, 004, and 102 peaks of dhcp $FeD_{1.0}$ are derived from the simulated profile shown in Fig. 4c and listed in Table 2.

Discussion

Crystal structure of dhcp deuteride. The structural parameters optimized for the dhcp $FeD_{1.0}$ at 300 K and 4.2 GPa are in agreement with those reported for the dhcp deuteride quenched at 90 K and 0.1 MPa[6]. The D atoms are located at the off-center positions displaced by $\delta z \sim 0.005c$ from the O-site centers along the *c*-axis. The stacking sequence of the Fe planes contains the hcp-stacking faults, as described by a 0.12 occupancy of Fe atoms at the f_{def}-defect positions. The values of δz and f_{def} are close to $0.007c$ and 0.155, respectively, of the quenched specimen. The off-center displacement and the stacking fault are removed in the dhcp solid solutions at high temperatures. In dhcp $FeD_{0.68(1)}$ at 673 K and 6.1 GPa, neither Fe nor D atoms occupy the defect positions, and the positions of D atoms still slightly deviate from the center of the octahedral site.

The off-center displacement is attributed to the repulsive interactions between the interstitial D atoms[6]. As known as the empirical 2.1-Å rule – dissolved H atoms in metals cannot approach each other within 2.1-Å in metal hydrides[36], because there are strong long-range repulsive interactions between interstitial H atoms. The nearest neighboring D–D distance is calculated as 2.18 Å (close to the critical value) for the D atoms, when assumed to occupy exactly the center positions of the face-shared octahedra. The displacement of D atoms from

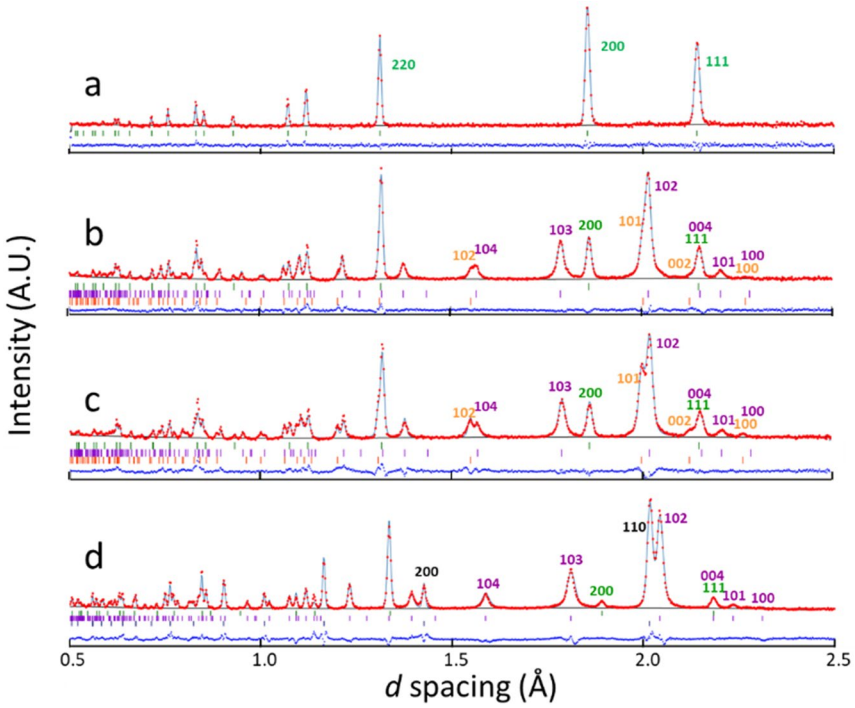

Figure 3. Powder neutron diffraction profiles of FeD_x measured at the following: (**a**) 1023 K and 6.1 GPa, (**b**) 673 K and 6.1 GPa, (**c**) 603 K and 4.8 GPa, and (**d**) 300 K and 4.2 GPa. Solid lines indicate diffraction profiles simulated using Z-Rietveld[35]. Blue lines indicate differences between the experimental (dots) and simulated (curves) profiles. Reflection indices and tick marks of Bragg peaks are shown in green, purple, orange and black for fcc, dhcp and hcp FeD_x and bcc Fe, respectively.

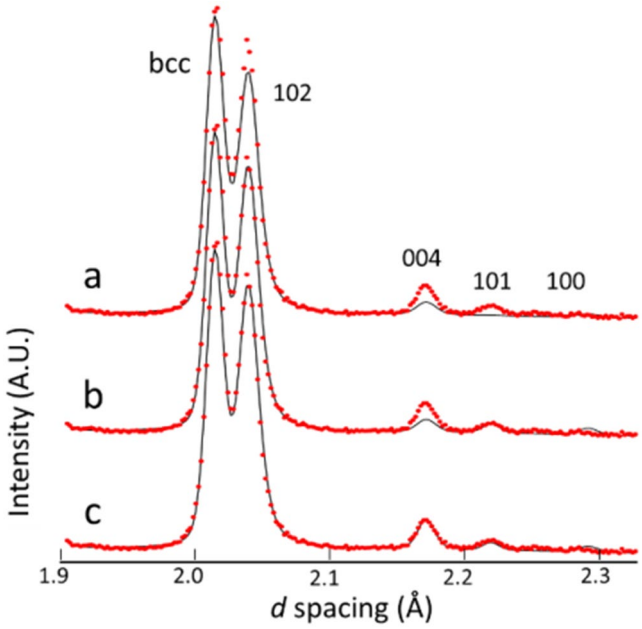

Figure 4. Diffraction profile at 300 K–4.2 GPa in the *d*-spacing range from 1.7 to 2.4 Å (red crosses). The profile was simulated (**a**) without a magnetic order, (**b**) with the out-of-plane model, and (**c**) with the in-plane model. Reflection indices denote the major peaks of dhcp deuteride.

the centers by $\delta z = 0.0053c$ (0.045 Å) increases the D–D distance to 2.27 Å, significantly greater than the critical value. As a result, some reduction in repulsive energy is expected.

h k l	I_{nuc}	I_{mag}	$I_{mag}/(I_{nuc}+I_{mag})$
1 0 0	1.37	0.67	0.329
1 0 1	0.12	3.12	0.962
0 0 4	3.95	5.26	0.571
1 0 2	100	9.99	0.091

Table 2. Nuclear (I_{nuc}) and magnetic scattering (I_{mag}) components of the 100, 101, 004, and 102 reflections of dhcp $FeD_{1.0}$ with the in-plane model. Each value isnormalized by $I_{nuc} = 100$ for the 102 peak.

The removal of atomic displacement in the solid solution is attributed to the partial release of the D atoms from the interstitial sites of the dhcp metal lattice. The D-content x decreased from 1.0 at 300 K to 0.68(1) at 673 K, and a third of the O sites became empty. All D atoms form nearest neighbor-pairs in $FeD_{1.0}$, whereas roughly half of the D atoms form pairs in the solid-solution $FeD_{0.68(1)}$ (the pairing ratio can be calculated by a square of the O-site occupancy of 0.68). The reduction in repulsive energy thus bring the D atoms back to the centers of octahedra. Another possible driving force for centering the D atoms is the thermal vibrations of the D atoms enhanced at high temperatures. The atomic displacement parameter B of the D atoms increased from 0.91 to 2.15 Å^2 as the temperature increased from 300 to 673 K. This value is almost twice as large as the 1.20 Å^2 for the H atoms in the dhcp FeH quenched at 300 K and 0.1 MPa, where no off-center displacement of H atoms was observed despite the full occupation of the O sites by H atoms[6].

The regular dhcp stacking sequence of the Fe planes gradually recovers with elevating temperature. The occupancy of the Fe atoms at the defect sites f_{def}, which represents the stacking fault degree, decreases from 0.123 at 300 K to 0.018 at 673 K via 0.043 at 603 K. This continuous variation with temperature contrasts the abrupt centering of the D atoms at 673 K. The atomic displacement parameter of the Fe atoms gradually increased from 0.33 to 0.74 Å^2 as the temperature increased from 300 to 673 K. Recovery of the regular stacking sequence appears unrelated to the centering of the D atoms and would be driven by the thermal activation of Fe atomic motions.

Magnetic structure of dhcp deuteride. The in-plane magnetic ordering determined for the dhcp $FeD_{1.0}$ is consistent with that proposed for dhcp $FeH_{1.0}$ in the early theoretical study[26]. The in-plane ordering of magnetic moments, proposed as a stable magnetic structure by the DFT calculations, is experimentally confirmed by the present NPD study. The calculations also predicted the magnetic moments of 1.90 and 2.08 μ_B/Fe-atom at sites 2*a* and 2*c*, respectively[26]. In fact, two distinct values of hyperfine fields were correspondingly observed by MB spectroscopy[30–34]. In the present structure refinement, the magnetic moment of 2.11(6) μ_B/Fe-atom is obtained under an assumption of one equivalent magnetic moment for the two sites. This value is slightly larger than the calculated moments and slightly less than the experimental moment of 2.22 μ_B/Fe-atom for dhcp FeH_x, that was measured for $0.65 \leq x \leq 0.81$ at temperatures of 4.2–80 K at ambient pressure[7,29]. The magnetic moment tends to increase with both decreasing T and x[27]. The value of 2.11(6) μ_B/Fe-atom of the dhcp $FeD_{1.0}$ at 300 K can be interpreted in terms of these T and x dependencies.

The large magnetic moment of the dhcp $FeD_{1.0}$ suggests a high critical temperature, Curie temperature T_c, for its ferromagnetic–paramagnetic transition upon temperature elevation. High T_c is expected from the temperature-dependence of the magnetization measured for the quenched dhcp FeH_x[29]. However, the measured temperature range of 4.2–80 K is too limited to estimate a T_c most likely far above room temperature. Pure iron, bcc Fe, has a magnetic moment of 2.218 μ_B/Fe-atom at 0 K and 0.1 GPa and undergoes a magnetic transition at 1043 K. The dhcp deuteride with a comparable magnetic moment is hence expected to exhibit a corresponding T_c of around 1000 K. Unfortunately, the magnetic moment was not determined for the dhcp solid solutions at high temperatures because observation of the magnetic scattering peaks was hindered by the rather intense peaks from the coexisting fcc FeD_x. The variation of T_c with x is essential for understanding the ferromagnetism in relation to the volume expansion and electron doping caused by dissolved D atoms. NPD investigation of dhcp deuteride, including solid solution states at high temperatures and high pressures, is a future research subject.

Methods

Reagent-grade pure iron flakes (purity: 99.9%) with a lateral particle size <100 μm and a thickness <20 μm were used as a starting material. A compacted Fe disc 3 mm in diameter and 2.5 mm in height was prepared by pressing the flakes in a piston–cylinder-type mold. The Fe disc was placed at the center of a NaCl capsule 5.5 mm in outer diameter and 8.2 mm in height, along with the internal deuterium source of AlD_3 (isotopic purity: 96 atom% D) pellets, placed above and below the disc. An excess amount of AlD_3 (Fe/D molar ratio of ~1.5) was charged into the cell to form Fe deuteride with equilibrium-D compositions during NPD measurements. The NaCl capsule containing the Fe disc and AlD_3 pellets was inserted into a cylindrical graphite heater and embedded in a pressure-transmitting medium (15-mm edge cube) made of MgO with a 5% Cr_2O_3 weight.

The high-pressure cell containing the Fe disc and AlD_3 pellets was first pressurized to ~6 GPa at 300 K and then heated to 1023 K. During heating, the AlD_3 pellets decomposed to provide a D_2 fluid, which dissolved into the Fe specimen to form fcc FeD_x. After confirming the deuteride formation at 1,023 K and 6.1 GPa by NPD diffraction, we lowered the temperature stepwise to 300 K for NPD measurements. Diffraction profiles were collected at four T–P points (Fig. 1), with an exposure time from 2 to 6 h, using a neutron source operating at a proton beam power of 300 kW.

The cell assembly and high-pressure apparatus used in the NPD measurements were described in detail in a previous paper[14]. Diffraction profiles were collected at the "PLANET" beamline at the Japan Proton Accelerator Research Complex (J-PARC), Tokai, Japan[37,38].

Data availability

All data supporting the findings of this study are available within the paper and Methods. The crystallographic data are available from the corresponding authors upon request.

Received: 24 March 2020; Accepted: 22 May 2020;
Published online: 18 June 2020

References

1. Fukai, Y. *The Metal–Hydrogen System* 2nd edn (Springer-Verlag, 2005).
2. Antonov, V. E., Belash, I. T. & Ponyatovsky, E. G. T-P phase diagram of the Fe-H system at temperatures to 450 C and pressures to 6.7 GPa. *Scr. Metal.* **16**, 203–208 (1982).
3. Badding, J. V., Hemley, R. J. & Mao, H. K. High-pressure chemistry of hydrogen in metals: *In situ* study of iron hydride. *Science* **253**, 421–424 (1991).
4. Yamakata, M., Yagi, T., Utsumi, W. & Fukai, Y. *In situ* X-ray observation of iron hydride under high pressure and high temperature. *Proc. Japan Acad.* **68B**, 172–176 (1992).
5. Fukai, Y., Yamakata, M. & Yagi, T. Some high-pressure experiments on the Fe–H system. *Z. Phys. Chem.* **179**, 119–123 (1993).
6. Antonov, V. E. *et al*. Neutron diffraction investigation of the dhcp and hcp iron hydrides and deuterides. *J. Alloys Compd.* **264**, 214–222 (1998).
7. Antonov, V. E. *et al*. High-pressure hydrides of iron and its alloys. *J. Phys. Condens. Matter* **14**, 6427–6445 (2002).
8. Fukai, Y., Mori, K. & Shinomiya, H. The phase diagram and superabundant vacancy formation in Fe–H alloys under high hydrogen pressures. *J. Alloys Compd.* **348**, 105–109 (2003).
9. Hirao, N., Kondo, T., Ohtani, E., Takemura, K. & Kikegawa, T. Compression of iron hydride to 80 GPa and hydrogen in the Earth's inner core. *Geophy. Res. Lett.* **31**, L06616 (2004).
10. Hiroi, T., Fukai, Y. & Mori, K. The phase diagram and superabundant vacancy formation in Fe–H alloys revisited. *J. Alloys Compd.* **404–406**, 252–255 (2005).
11. Fukai, Y. & Sugimoto, H. Formation mechanism of defect metal hydrides containing superabundant vacancies. *J. Phys.: Condens. Matter* **19**, 436201 (2007).
12. Sakamaki, K. *et al*. Melting phase relation of FeH_x up to 20 GPa: Implication for the temperature of the Earth's core. *Phys. Earth Planet. Inter.* **174**, 192–201 (2009).
13. Narygina, O. *et al*. X-ray diffraction and Mössbauer spectroscopy study of fcc iron hydride FeH at high pressures and implications for the composition of the Earth's core. *Earth Planet. Sci. Lett.* **307**, 409–414 (2011).
14. Machida, A. *et al*. Site occupancy of interstitial deuterium atoms in face-centred cubic iron. *Nat. Commun.* **5**, 5063 (2014).
15. Pépin, C. M., Dewaele, A., Geneste, G., Loubeyre, P. & Mezouar, M. New Iron Hydrides Under High Pressure. *Phys. Rev. Lett.* **113**, 265504 (2014).
16. Saitoh, H., Machida, A., Sugimoto, H., Yagi, T. & Aoki, K. P-V-T relation of the Fe-H system under hydrogen pressure of several gigapascals. *J. Alloys Compd.* **706**, 520–525 (2017).
17. Pépin, C. M., Geneste, G., Dewaele, A., Mezouar, M. & Loubeyre, P. Synthesis ofFeH5: A layered structure with atomic hydrogen slabs. *Science* **357**, 382 (2017).
18. Machida, A. *et al*. Hexagonal Close-packed Iron Hydride behind the Conventional Phase Diagram. *Scientific Reports.* **9**, 12290 (2019).
19. Ikuta, D. *et al*. Interstitial hydrogen atoms in face-centered cubic iron in the Earth's core. *Scientific Reports* **9**, 7108 (2019).
20. Antonov, V. E. *et al*. Solubility of deuterium and hydrogen in fcc iron at high pressures and temperatures, Phys. *Rev. Materials* **3**, 113604 (2019).
21. Mitsui, T. & Hirao, N. Ultrahigh-pressure study on the magnetic state of iron hydride using an energy domain synchrotron radiation 57Fe Mössbauer spectrometer. *Maer. Res. Soc. Symp. Proc.* **1262**, 1262-W06-09 (2010).
22. Ishimatsu, N. *et al*. Magnetic state in iron hydride under pressure studied by X-ray magnetic circular dichroism at the Fe K-edge. *Maer. Res. Soc. Symp. Proc.* **1262**, 1262-W04-02 (2010).
23. Ishimatsu, N. *et al*. Hydrogen-induced modification of the electronic structure and magnetic states in Fe, Co, and Ni monohydrides. *Phys. Rev. B* **86**, 104430 (2012).
24. Elsässer, C. *et al*. Ab initio study of iron and iron hydride: II. Structural and magnetic properties of close-packed Fe and FeH. *J. Phys.: Condens. Matter* **10**, 5113–5129 (1998).
25. Pronsato, M. E., Brizuela, G. & Juan, A. The electronic structure of iron hydride. *J. Phys. Chem. Solids* **64**, 593–597 (2003).
26. Tsumuraya, T. & Matsuura, Y. Shishidou, & Oguchi, T. First-Principles Study on the Structural and Magnetic Properties of Iron Hydride. *J. Phys. Soc. Jpn.* **81**, 064707 (2012).
27. León, A., Velásquez, E. A., Mejía-López, J. & Vargas, P. Ab initio study of the magnetic behavior of metal hydrides: A comparison with the Slater-Pauling curve. *Computational Materials Science* **141**, 122–126 (2018).
28. Gomi H., Fei1 Y. & Yoshino T. The Effects of Ferromagnetism and Interstitial Hydrogen on the Physical Properties of hcp and dhcp FeHx: Implications for the Density and Magnetism of a Hydrogen-bearing Core, *Lunar and Planetary Science XLVIII*, 1775 (2017).
29. Antonov, V. E., Belash, I. T., Ponyatovsky, E. G., Thiessen, V. G. & Shiryaev, V. I. Magnetization of Iron Hydride. *Phys. Stat. Sol. (a)* **65**, K43–K48 (1981).
30. Wordel, R. R. *et al*. Mössbauer study of iron hydride produced under high pressure. *Hyperfine Interactions* **28**, 1005–1008 (1986).
31. Antonov, V. E. *et al*. Crystal Structure and Magnetic Properties of High-Pressure Phases in the Fe-H and Fe-Cr-H Systems. *Int. J. Hydrogen Energy* **14**, 371–377 (1989).
32. Schneider, G. *et al*. Mössbauer study of hydrides and deuterides of iron and cobalt. *J. Less-Common Met.* **172–174**, 333–342 (1991).
33. Choe, I., Ingalls, R., Brown, J. M., Sato-Sorensen, Y. & Mills, R. Mössbauer studies of iron hydride at high pressure. *Phys. Rev. B* **44**, 1–4 (1991).
34. Antonov, V. E. *et al*. High-pressure hydrides of iron and its alloys. *J. Phys.: Condens. Matter* **14**, 6427–6445 (2002).
35. Oishi, R. *et al*. Rietveld analysis software for J-PARC. *Nucl. Instrum. Methods. Phys. Res. Sect. A* **600**, 94–96 (2009).
36. Westlake, D. G. Stoichiometries and interstitial site occupation in the hydrides of ZrNi and other isostructural intermetallic compounds. *J. Less-Common Mel.* **75**, 177–185 (1980).
37. Sano-Furukawa, A. *et al*. Six-axis multi-anvil press for high-pressure, high temperature neutron diffraction experiments. *Rev. Sci. Instrum.* **85**, 113905 (2014).
38. Hattori, T. *et al*. Design and performance of high-pressure PLANET beamline at pulsed neutron source at J-PARC. *Nucl. Instrum. Methods Phys. Res. Sect. A* **780**, 55–67 (2015).

Acknowledgements
Neutron diffraction experiments were performed under proposal no. 2017B0127 in J-PARC. High-pressure hydrogenation conditions of iron were preliminary investigated using *in situ* synchrotron radiation X-ray diffraction at BL14B1, SPring-8 (2015A3602 and 2015B3602). This work was supported by the JAEA under the remit of "Nanotechnology Platform" of MEXT, Japan (grant number JPMXP09A20QSA15AE0033), the Grants-in-aid for Scientific Research of Japan Society for the Promotion of Science (grant numbers 24241032, 25220911 and 18H05224).

Author contributions
H.S., R.I.-O., T.H., A.S.-F., K.F. and K.A. performed the high-pressure neutron diffraction experiments. T.S. and S.O. prepared AlD_3. A.M. and K.A. analysed the neutron diffraction data. H.S. and K.A.wrote the manuscript. K.A. directed this study.

Competing interests
The authors declare no competing interests.

Additional information
Correspondence and requests for materials should be addressed to H.S. or K.A.

Reprints and permissions information is available at www.nature.com/reprints.

Publisher's note Springer Nature remains neutral with regard to jurisdictional claims in published maps and institutional affiliations.